ELSEVIER

Journal of Magnetism and Magnetic Materials 241 (2002) 447–452

Journal of magnetism and magnetic materials

www.elsevier.com/locate/jmmm

Magnetic nanostructure fabrication by soft lithography and vortex-single domain transition in Co dots

S.P. Li[a,*], M. Natali[a], A. Lebib[a], A. Pépin[a], Y. Chen[a], Y.B. Xu[b]

[a] *Laboratoire de Microstructures et de Microélectronique (CNRS), 196 Avenue H. Ravera, 92225 Bagneux Cedex, France*
[b] *Cavendish Laboratory, Maldingley Road, Cambridge CB3 OHE, UK*

Received 26 April 2001; received in revised form 19 June 2001

Abstract

Micron/nano scale Co dot and wire arrays have been fabricated by soft lithography patterning with a resolution of 100 nm. Magneto-optic Kerr effect magnetometry combined with micromagnetic calculation is used to study, in detail, the vortex-single domain transition in the Co dots. A metastable single-domain state, which is stabilized by a local minimum energy induced by vortex nucleation, is demonstrated.

PACS: 75.50.Gg; 78.20.Ls; 75.60.−d; 85.42.+m

Keywords: Magnetic structures; Soft lithography; Magneto-optics

1. Introduction

Patterned magnetic structures are important not only for practical application but also for fundamental understanding of micromagnetics. For example, quantized magnetic disks can overcome the storage density limit of conventional thin-film magnetic disks by several orders of magnitude [1,2]. Reducing the lateral dimensions of magnetic film to values comparable to the critical lengths of magnetism, such as domain wall width or minimum domain size, would be helpful to obtain new information on the micron and nanomagnetic intrinsic processes [3,4]. Various methods such as electron beam lithography [4,5], X-ray lithography [6], nanoimprint [2,7], interference [8] as well as mechanical plow techniques [9] have been used to pattern magnetic micron and nanostructures. In this work, we report on a new approach of microcontact printing to fabricate magnetic microstructures, which has not been reported so far. The magnetization reversal properties of these magnetic structures were studied by magneto-optic Kerr effect (MOKE) and micromagnetic calculation. A energetically metastable single-domain state in the Co dots which involves vortex nucleation is demonstrated.

2. Experimental method

The micro-contact printing uses an elastomeric stamp to transfer thiol molecules to an appropriate

*Corresponding author. Present address: Nanoscale Science Laboratory, Engineering Department, University of Cambridge, Trumpington Street, Cambridge CB2 1PZ, UK. Tel.: +44-1223-332608; fax: +44-1223-332662.

E-mail address: sl252@eng.cam.ac.uk (S.P. Li).

0304-8853/02/$ - see front matter
PII: S0304-8853(01)00441-3

surface by monolayer self-assembling [10,11]. Our stamps were prepared by casting and curing of polymer mixture (VDT-731 and HMS-301) against patterned masters obtained by electron beam lithography and reactive ion etching of SiO_2. The stamp preparation process was well documented in reference [12]. In short, we use VDT-731 and HMS-301 at a rate of 3.4 : 1, with 5 ppm platinum catalyst, and 0.1% modulator (2,4,6,8-tetramethyl-tetravinylcyclotetrasiloxane).

A typical fabrication process in our experiment is schematically shown in Fig. 1. We first spin coat a standard lithography resist such as polymethylmethacrylate (PMMA) on Si wafers with a native oxide layer, followed by a prebake at 200°C for 30 min. Then, a 20 nm thick Au was sputtered on the PMMA layer. Finally, a self-assembled monolayer (SAM) pattern is obtained on the gold surface by micro-contact printing. To improve the adhesion between gold and PMMA resist and wet etching quality, a 5 nm Ti was introduced before gold deposition. The ink solution we used is 0.01 M eicosanethiol ($C_{20}H_{41}SH$) in ethanol. The stamps were wetted with these thiol solutions for 1 min and then slightly washed use ethanol and dried in a flow of dry nitrogen. The stamps were carefully brought in contact with the sample for 15 s. After removal of the stamps, the samples were etched in aqueous solution of 1 M KOH, 0.1 M $Na_2S_2O_3$, 0.01 M $K_3Fe(CN)_6$, and 0.001 M $K_4Fe(CN)_6$ for 8 min, until the parts of the gold which were not protected by SAM layer were completely removed. Then, the samples were placed in a reactive ion etching (RIE) chamber to etch Ti and PMMA with SF_6 and O_2 plasma, respectively. Finally, the resulted PMMA resist profiles were used for lift-off of Co. The patterning of PMMA using micro-contact has some advantages as compared with electron-beam and X-ray lithography in terms of mass production and cost, etc.

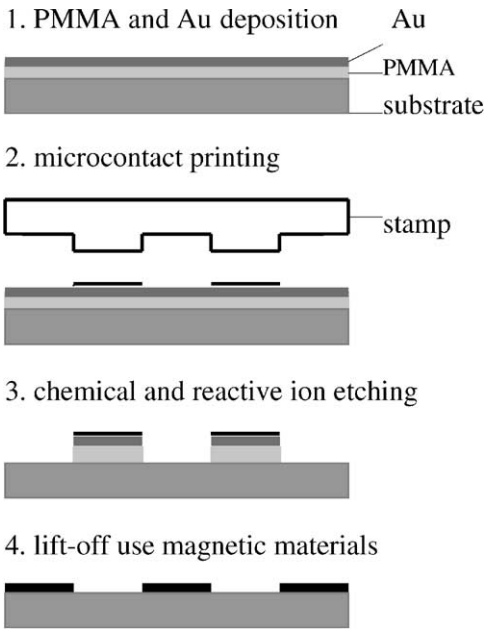

Fig. 1. Schematic illustration of the soft lithography used to fabricate magnetic structures.

3. Results and discussion

A high uniformity over large area magnetic structures with 200 nm resolution can be easily obtained (Figs. 2a and b). The smallest Co dots we obtained are 100 nm in diameter (Fig. 2c). Co structures of different thicknesses up to 60 nm were obtained. In particular, we have characterized magnetic properties of circular Co dots for various feature sizes and thickness. The periods of patterned dots in our investigated samples were selected to be equal or larger than twice that of the dot diameter. The interdot dipolar coupling is often believed to be negligible when the ratio of separation to the diameter is large than one [13]. The unpatterned films had a $\sim$60 Oe coercivity and a small uniaxial in plane anisotropy which is induced by stray magnetic field during growth. Fig. 3 presents typical magnetic hysteresis loops obtained from 200 nm diameter Co dots with thickness 50, 15, and 10 nm, respectively. As expected, a strong thickness dependence was observed. The zero remanence in loop (a) is characteristic of formation of a vortex configuration of magnetic moments [14,15], while the square loop (c) is characteristic of single-domain behaviour and magnetization reversal occurs by all magnetic moments rotating coherently [16]. In the intermediate case, a double switch-like with high

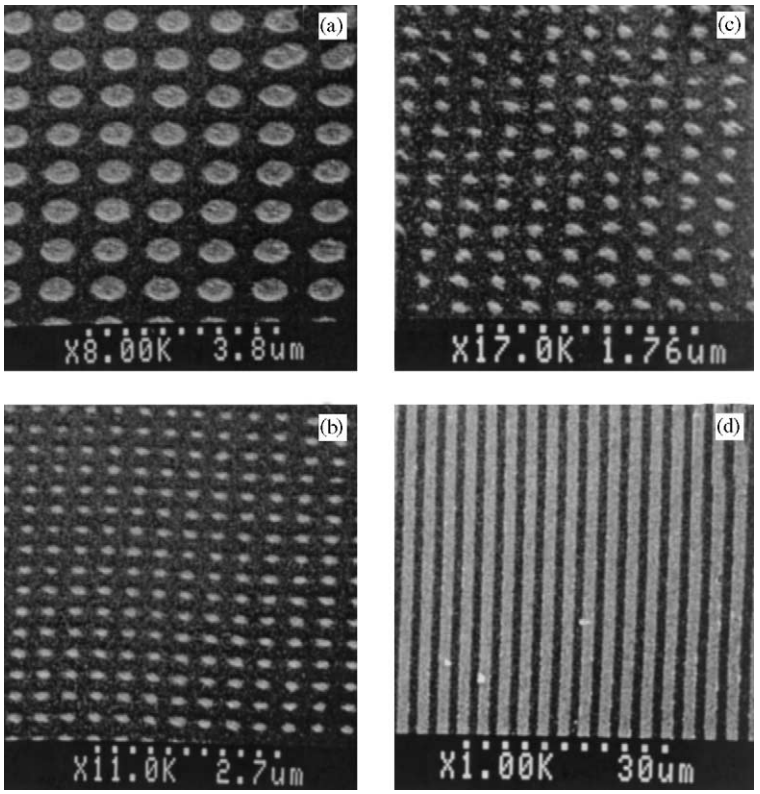

Fig. 2. SEM images of 50 nm thick Co structures obtained by micro-contact printing and a subsequent lift-off; (a–c)—disk structures with diameters of 500, 200, and 100 nm, respectively, and (d)—wire structure with 1.5 μm width and separation. All the images were taken at 60° with respect to the sample surfaces.

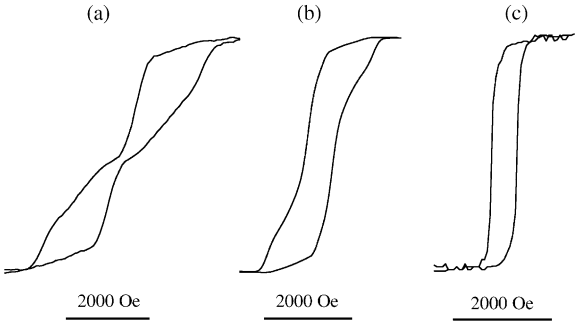

Fig. 3. Magnetic hysteresis loops measured on 200 nm diameter Co disks with thicknesses: 50 nm (a), 15 nm (b), and 10 nm (c).

remanence hysteresis loop can be found (loop (b)). Since anisotropy energy is negligible the magnetization configuration is determined by the balance between the exchange (E_{ex}) and demagnetized (E_d) energy which is controlled by the film thickness and diameter. By competition of these two kinds of energies, there exist a transition from vortex state into a single-domain state upon lowering both the disk diameter and thickness [17]. For vortex state, a fluxclosure configuration is formed which involves a large amount of exchange energy. In contrast, the single-domain state involves a large amount of demagnetized energy produced by the surface charge at the edges. Upon decreasing the film thickness at constant diameter, the demagnetized energy is reduced and eventually the total energy becomes lower than that of the vortex state and the single-domain state is more stable at lower thickness. Actually, the experimental vortex-single domain state phase transition boundary does not precisely agree with theoretical calculation; it occurs on higher thickness than that

is theoretically predicted [17]. Therefore, there must be another dynamic process to resist the vortex formation in a thickness range where vortex magnetization configuration is a lower energy state, and render a metastable single-domain state. In order to verify this, suppose we have performed a numerical micromagnetic calculation on single magnetically isolated dot using the publicly available 2D code OOMMF [18]. The material parameters are saturation magnetization $M_s = 1400\,\mathrm{emu/cm^3}$, exchange constant $A_{ex} = 1.4\times 10^{-6}\,\mathrm{erg/cm}$, zero magnetocrystalline anisotropy, and damping parameter $\alpha = 1.0$ which determines the relaxation of the magnetization into its local effective equilibrium field direction [19]. The mesh size was chosen to be 5 nm. Fig. 4 shows the energy distribution as a function of external field (magnetization configuration) and calculated hysteresis loops for dots with thickness 50, 15 and 10 nm. Clearly, for the dots which give zero remanence hysteresis loop (Fig. 4a) there is a minimum of the total energy ($E_{tot} = E_{ex} + E_d$, the Zeeman energy is not enclosed as we discuss the field dependence) in the remanent state. In this case, the vortex magnetization configuration adopts ground state with no external field. With decreasing dot thickness, the location of ground state shifts in the direction of higher field and the remanent state corresponds to a high energy value (Fig. 4b). Such a stabilized remanent state with high energy must be in a local minimum and is an unstable state. To clarify this, Fig. 5 shows a large scale plot of the energy curves of Fig. 4b around remanent state which are indicated by arrows. Indeed, a minimum of total energy can be viewed in the remanent state (Fig. 5c). The origin of the formation of this local minimum can be understood from the evolution of exchange and demagnetized energy with the magnetization configuration. Complete magnetization reversal must take place via vortex nucleation, vortex movement, and annihilation process [8]. Though the vortex magnetization configuration is energetically favourable, in the moment of vortex nucleation, a local high disorder of magnetization will be introduced, and in turn exchange energy is increased (Fig. 5a). This increased exchange energy cannot be compensated by the decreased demagnetized energy (Fig. 5b) in this thickness range and an energy barrier is formed. This barrier defines a local energy minimum in the remanent state where a single domain magnetization configuration is trapped. To adopt the ground vortex state, an external field is required to cross the energy barrier. For thicker dots, when the vortex magnetization configuration is formed, the decrease in demagnetized energy is therefore large enough to compensate the increased exchange energy induced by the vortex nucleation and a vortex state can be adopted

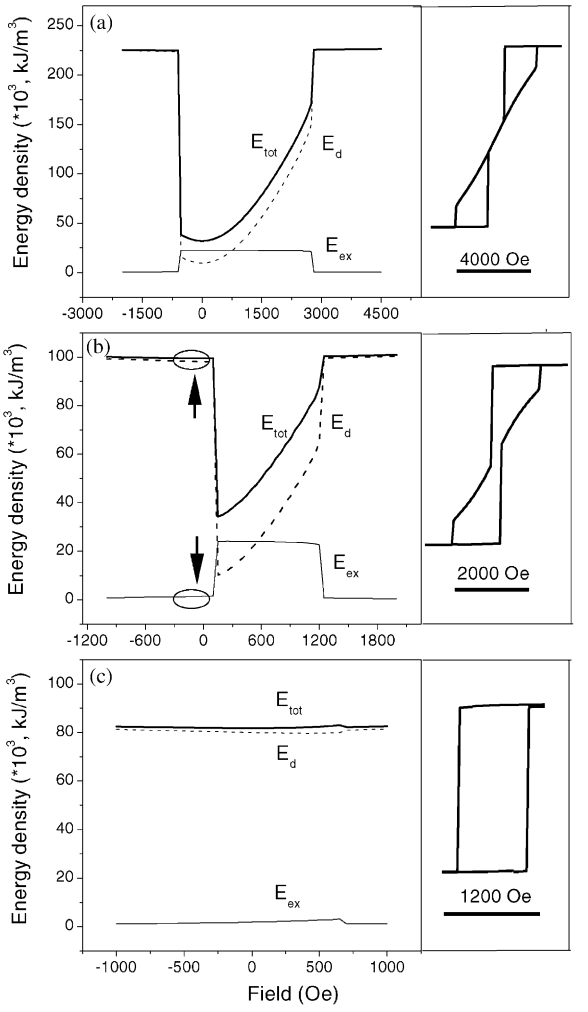

Fig. 4. Energy distribution as a function of external field and calculated hysteresis loops for 200 nm disks with thicknesses: 50 nm (a), 15 nm (b), and 10 nm (c).

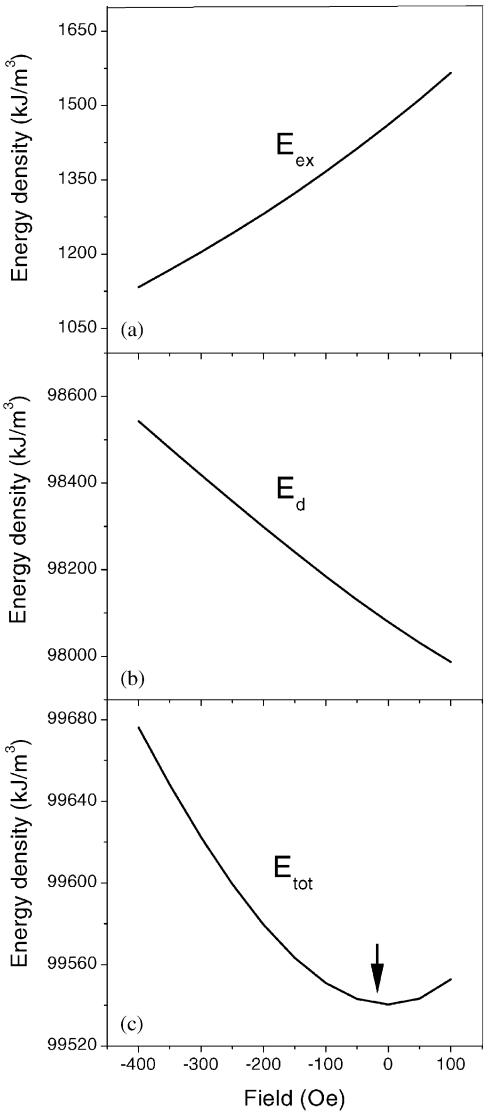

Fig. 5. A plot with large scale for the region indicated in Fig. 4b. (a) Exchange energy; (b) demagnetized energy; and (c) total energy. The arrow in (c) indicates a local energy minimum at the remanent position.

without any external energy (in the remanent state). With further decrease in dot thickness, the magnetization reversal occurs by all magnetic moments rotating coherently, while both exchange and demagnetized energy remain almost constant with external field (Fig. 4c).

4. Conclusion

We have successfully demonstrated the patterning of magnetic micron/nano scale structures with 100 nm resolution using soft lithography. Magneto-optical Kerr effect hysteresis loops and micromagnetic calculation were used to study the vortex-single domain transition in Co dots. Except for the energy balance between the vortex and single-domain magnetization configuration, a new mechanism involving vortex nucleation is proposed. In an appropriate thickness range, a local energy minimum induced by vortex nucleation can stabilize a single-domain state.

Acknowledgements

We gratefully acknowledge the financial support of the European Commission under the ESPRIT program #22464, 'MASSD'.

References

[1] S.Y. Chou, M.S. Wei, P.R. Krauss, P.B. Fischer, J. Appl. Phys. 76 (1994) 6673.
[2] Wei Wu, Bo Cui, Xiao-yun Sun, Wei Zhang, Lei Zhuang, Linshu Kong, Stephen Y. Chou, J. Vac. Sci. Technol. B 16 (1998) 3825.
[3] M. Hehn, K. Ounadjela, J. Bucher, F. Rousseaux, D. Decanini, B. Bartenlian, C. Chappert, Science 272 (1996) 1782.
[4] S.P. Li, D. Peyrade, M. Natali, A. Lebib, Y. Chen, U. Ebels, L.D. Buda, K. Ounadjela, Phys. Rev. Lett. 86 (2001) 1102.
[5] Y. Otani, B. Pannetier, J.P. Nozieres, D. Givord, J. Magn. Magn. Mater. 126 (1993) 622.
[6] F. Rousseaux, D. Decanini, F. Carcenac, E. Cambril, M.F. Ravet, C. Chappert, N. Bardou, B. Bartenlian, P. Veillet, EIPB-95, 1995.
[7] Lebib, S.P. Li, M. Natali, Y. Chen, J. Appl. Phys. 89 (2001) 3892.
[8] C. Pike, A. Fernandez, J. Appl. Phys. 85 (1999) 6668.
[9] S.P. Li, A. Lebib, D. Peyrade, M. Natali, Y. Chen, Appl. Phys. Lett. 77 (2000) 2743.
[10] Y. Xia, G.M. Whitesides, Angew. Chem. Int. Ed. 37 (1998) 550.
[11] H.A. Biebuyck, N.B. Larsen, E. Delamarche, B. Michel, IBM J. Res. Dev. 41 (1997) 159.
[12] H. Schmid, B. Michel, Macromolecules, Preprint, IBM Research Division, Zurich Research Laboratory.

[13] A.O. Adeyeye, J.A.C. Bland, C. Daboo, D.G. Hasko, Phys. Rev. B 56 (1997) 3265.
[14] T. Shinjo, T. Okuno, R. Hassdorf, K. Shigeto, T. Ono, Science 289 (2000) 930.
[15] A. Fernandez, C.J. Cerjan, J. Appl. Phys. 87 (2000) 1395.
[16] E.C. Stoner, E.P. Wohlfarth, Philos. Trans. R. Soc. London A 240 (1948) 74.
[17] R.P. Cowburn, D.K. Koltsov, A.O. Adeyeye, M.E. Welland, D.M. Tricker, Phys. Rev. Lett. 83 (1999) 1042.
[18] http://math.nist.gov/oommf.
[19] M.R. Scheinfein, J.L. Blue, J. Appl. Phys. 69 (1991) 7740.